

1 **Increase of dissolved inorganic carbon and decrease of pH in near surface**
2 **waters of the Mediterranean Sea during the past two decades**

3

4

5 Liliane. Merlivat ^a, Jacqueline. Boutin ^a, David. Antoine ^{b,c}, Laurence. Beaumont ^d, Melek.
6 Golbol ^b, Vincenzo. Vellucci. ^b

7

8 ^a Sorbonne Universités (UPMC, Univ Paris 06)-CNRS-IRD-MNHN, LOCEAN Laboratory,
9 F-75005 Paris, France

10 ^b Sorbonne Universités (UPMC, Univ Paris 06)-CNRS, LOV, Observatoire Océanologique,
11 Villefranche-sur-Mer 06230, France

12 ^c Remote Sensing and Satellite Research Group, Department of Physics and Astronomy,
13 Curtin University, Perth, WA 6845, Australia

14 ^d Division Technique INSU-CNRS, 92195 Meudon Cedex, France

15

16 Corresponding author: L. Merlivat (merlivat@locean.upmc.fr)

17

18

19 **Abstract**

20 Two three-year-long time series of hourly measurements of the fugacity of CO₂ (fCO₂) in the
21 upper 10m of the surface layer of the northwestern Mediterranean Sea have been recorded by
22 CARIOCA sensors almost two decades apart, in 1995-1997 and 2013-2015. By combining
23 them with alkalinity derived from measured temperature and salinity, we calculate changes of
24 pH and dissolved inorganic carbon (DIC). DIC increased in surface seawater by ~ 25 μmol
25 kg⁻¹ and fCO₂ by 40 μatm, whereas seawater pH decreased by ~ 0.04 (0.0022 yr⁻¹). The DIC
26 increase is about 15% larger than expected from equilibrium with atmospheric CO₂. This
27 could result from the increase between the two periods in the frequency and intensity of
28 winter convection events. Likewise, it could be the signature of the contribution of the
29 Atlantic Ocean as a source of anthropogenic carbon to the Mediterranean Sea through the
30 strait of Gibraltar. Under this assumption, we estimate that the part of DIC accumulated over
31 the last 18 years represents ~30% of the total change of anthropogenic carbon since the

32 beginning of the industrial period.

33

34 **1 Introduction**

35 The concentration of atmospheric carbon dioxide (CO₂) has been increasing rapidly over
36 the 20th century and, as a result, the concentration of dissolved inorganic carbon (DIC) in
37 the near surface ocean increases, which drives a decrease in pH in order to maintain a
38 chemical equilibrium [Millero, 2007]. These changes have complex direct and indirect
39 impacts on marine organisms and ecosystems [Gattuso and Hansson, 2011]. Empirical
40 methods to estimate the anthropogenic CO₂ penetration in the ocean since the industrial
41 revolution have improved over the past few decades [Chen and Millero, 1979; Gruber et
42 al., 1996]; [Sabine et al., 2008]; [Touratier and Goyet, 2004; 2009; Woosley et al., 2016].
43 As the concentration of anthropogenic carbon, C_{ant}, cannot be distinguished from the
44 natural background of DIC through total DIC measurements, these methods are based on
45 the analysis of different chemical properties of the water column. Direct estimates of the
46 anthropogenic CO₂ absorption in the sea surface layers are difficult owing to the large
47 natural variability driven by physical and biological phenomena. [Bates et al., 2014] have
48 extracted the trend from the large variability, based on analysis of a long time series
49 (monthly or seasonal sampling). For the global surface ocean, [Lauvset et al., 2015] have
50 used the Surface Ocean CO₂ Atlas (SOCAT) database [Bakker et al., 2014] combined with
51 an interpolation method. The quantitative estimation of anthropogenic CO₂ storage in the
52 Mediterranean Sea based on experimental data is very inaccurate, of the order of a factor two
53 [Huertas et al., 2009; Touratier and Goyet, 2009]. In addition to the anthropogenic signal,
54 oceanic DIC can also be the signature of a strong interannual variability. In the North
55 Atlantic, for instance it has been shown that because of decadal variability it requires 25
56 years for the long-term trend to emerge [McKinley et al., 2011][McKinley et al.,
57 2011][McKinley et al., 2011][McKinley et al., 2011].

58 A high frequency sampling of the seawater carbon chemistry at the air-water interface over
59 extended periods of time is a way to detect a possible trend in DIC. In this paper we analyze
60 two three-year time series of hourly fugacity of CO₂, fCO₂, measured with autonomous
61 CARIOCA sensors [Copin-Montégut et al., 2004; Merlivat and Brault, 1995] in 1995-1997
62 and 2013-2015, at two very close locations in the northwestern Mediterranean Sea (Fig. 1).
63 Using measured fCO₂, temperature (T) and salinity (S), we derive the other variables of the

64 carbonate system (pH and DIC). The experimental setting is first described, and the recent
65 data obtained over the 2013-2015 period are presented. Combined with the 1995-1997
66 measurements previously published [Hood and Merlivat, 2001], we estimate the decrease of
67 pH and the increase of DIC. The results are discussed with respect to the contributions of the
68 exchange with atmospheric CO₂, to the possible impact of vertical mixing and to recent
69 estimates of the transport of anthropogenic carbon from the Atlantic Ocean over a 18 years
70 period.

71

72 2 Material and methods

73 2.1-The BOUSSOLE and DYFAMED sites

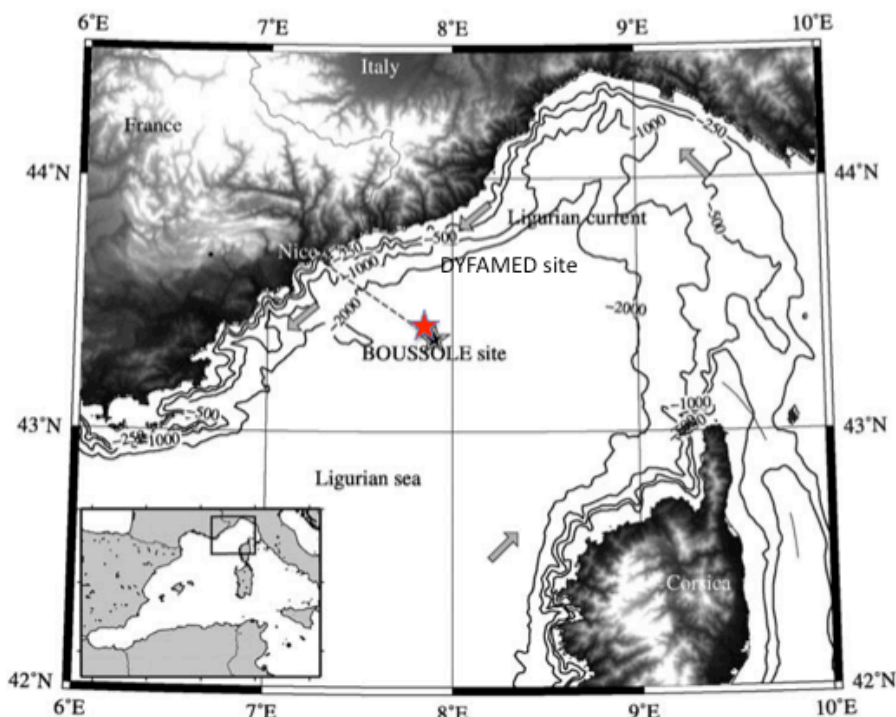


Fig. 1. The area of the northwestern Mediterranean Sea showing the southern coast of France, the island of Corsica, the main current branches (gray arrows), and the location of the DYFAMED site (red star) and the BOUSSOLE buoy (black star) in the Ligurian Sea.

74

75 Data collection was carried out at the BOUSSOLE site (43°22'N, 7°54'E) in 2013-2015
76 [Antoine *et al.*, 2008; Antoine. and others, 2006] and at the DYFAMED site (43°25'N,
77 7°52'E) in 1995-1997 [Marty *et al.*, 2002]. These sites are 3 nautical miles apart, both located
78 in the Ligurian Sea, one of the basins of the northwestern Mediterranean Sea (Fig.1). The
79 water depth is of ~2400 m. The prevailing ocean currents are usually weak (<20 cm s⁻¹),
80 because these sites are in the central area of the cyclonic circulation that characterizes the
81 Ligurian Sea. The two sites surrounded by the permanent geostrophic Ligurian frontal jet

82 flow are protected from coastal inputs [*Antoine et al.*, 2008; *Heimbürger et al.*, 2013; *Millot*,
83 1999]. Monthly cruises are carried out at the same location .

84

85 2.2- Analytical methods

86 At DYFAMED, fCO₂ measurements at 2 m depth were provided by an anchored floating
87 buoy fitted with a CARIOCA sensor. At BOUSSOLE, measurements were carried out from a
88 mooring normally dedicated to radiometry and optical measurements, and onto which two
89 CARIOCA sensors were installed. Both monitored fCO₂ hourly at 3 and 10 meters depth
90 (although only one of the two depths was equipped with a functional sensor at some periods);
91 S and T were monitored at the same two depths using a Seabird SBE 37-SM MicroCat
92 instrument. The CARIOCA sensors were adapted to work under pressure in the water column.
93 They were swapped about every 6 months, with serviced and calibrated instruments replacing
94 those having been previously deployed. The accuracy of CARIOCA fCO₂ measurements by
95 the spectrophotometric method based on the optical absorbance of a solution thymol blue
96 diluted in seawater is estimated at 2 μatm during both periods. [*Hood and Merlivat*, 2001]
97 have reported agreement between fCO₂ measured by CARIOCA buoys, similar to the one
98 deployed at DYFAMED, with ship based measurements, during a number of field programs,
99 with an accuracy of 2 μatm and a precision of 5 μatm .

100 At Boussole, newly designed fCO₂ sensors have been calibrated using in situ seawater
101 samples taken at 5 and 10 meters depth during the monthly servicing cruises to the mooring.
102 The total alkalinity, Alk , and DIC of the samples were determined by potentiometric titration
103 using a closed cell according to the method developed by [*Edmond*, 1970]. Certified
104 Reference Materials (CRMs) supplied by Dr. A.G. Dickson (Scripps Institution of
105 Oceanography, San Diego, USA) were used for calibration. The accuracy is estimated at 3
106 μmol kg⁻¹ for both DIC and Alk. fCO₂ is calculated using the dissociation constants of
107 Mehrbach refitted by Dickson and Millero [*Dickson and Millero*, 1987; *Mehrbach et al.*,
108 1973]. Error on fCO₂ derived from an individual sample is expected to be on the order of 5
109 μatm [*Millero*, 2007]. About 8 samples have been used to calibrate each CARIOCA sensor so
110 that the error on the absolute calibration of each fCO₂ CARIOCA sensor, is estimated at 1.8
111 μatm. In addition, we observe that the standard deviation of the difference between the
112 CARIOCA fCO₂ and fCO₂ computed with the monthly discrete samples (Fig. 2b) is equal to
113 4.4 μatm, consistent with the expected precision on CARIOCA fCO₂ of 5 μatm. Alk and S of
114 the 56 samples taken at BOUSSOLE are linearly correlated according the following
115 relationship :

116
$$\text{Alk} (\mu\text{mol kg}^{-1}) = 87.647 S - 785.5 \quad (1)$$

117 The standard deviation of the Alk data around the regression line is equal to $4.4 \mu\text{mol kg}^{-1}$
 118 ($r^2=0.89$).

119

120 **3 Results**

121 **3.1 The BOUSSOLE mooring (2013-2015) time series**

122 Temperature and $f\text{CO}_2$ were measured from February 2013 to February 2016. All seasons
 123 were well represented, with missing data only in May-July 2013. For some periods,
 124 simultaneous measurements were made at 3 and 10 m depth (Fig. 2, a, b, c).

125

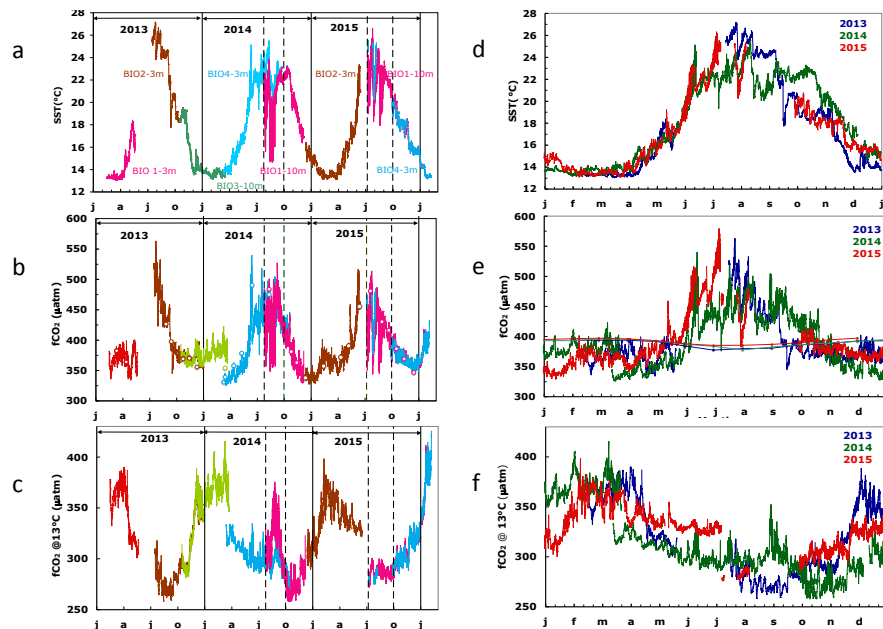


Fig.2. Interannual variability of CARIOCA data: a) T, b) $f\text{CO}_2$, c) $f\text{CO}_2@13^\circ\text{C}$. The dotted lines indicate the period affected by stratification and internal waves (July, 26th to October 1st, 2014 and July, 8th to October 1st, 2015). On 2(b), the open circles correspond to $f\text{CO}_2$ data derived from DIC and alkalinity measurements of samples taken at 5 and 10 meters. (d), (e), (f), seasonal variability. On 2(e), the thin lines indicate $f\text{CO}_{2\text{atm}}$. Note that the color code on (d), (e), (f) is different from (a), (b), (c).

126

127 The range of temperature (Fig. 2a) extends from 13°C in winter up to 27°C in summer,
 128 followed by progressive cooling in fall. The coldest temperature, 13°C , results from the
 129 winter vertical mixing with the deeper Levantine Intermediate Water, LIW, marked by
 130 extrema in temperature and salinity [Copin-Montegut and Begovic, 2002]. Temperature
 131 provides the main control of the seasonality of $f\text{CO}_2$, from $350 \mu\text{atm}$ to more than $550 \mu\text{atm}$ in
 132 summer 2013 (Fig. 2b). The fugacity of CO_2 in seawater is a function of temperature, DIC,
 133 alkalinity, salinity and dissolved nutrients. In the oligotrophic surface waters of the
 134 Mediterranean sea, this last effect should be negligible. Temperature and DIC have the

135 strongest influences. By normalizing $f\text{CO}_2$ to a constant temperature, the thermodynamic
136 effect can be removed and changes in $f\text{CO}_2$ resulting from changes in DIC can be more easily
137 identified. Figure 2c shows the variability of $f\text{CO}_2$ normalized to the constant temperature of
138 13°C , ($f\text{CO}_2@13$), using the equation of [Takahashi *et al.*, 1993]. The underlying processes
139 that govern the seasonal variability of $f\text{CO}_2@13$ are successively winter mixing, biological
140 activity (organic matter formation and remineralization) and deepening of mixed layer in fall
141 [Begovic and Copin-Montegut, 2002; Hood and Merlivat, 2001]. Biology accounts for the
142 decline in $f\text{CO}_2@13$ observed from March-April to late summer; the ensuing increase of
143 surface $f\text{CO}_2@13$ is associated with the deepening of the mixed layer in the fall or convection
144 in winter as the vertical distribution of $f\text{CO}_2@13$ at DYFAMED shows a maximum in the 50-
145 150 m layer where a large remineralization of organic matter occurs, the productive layer
146 being mostly between 0 and 40 m [Copin-Montegut and Begovic, 2002]. The contribution of
147 air-sea exchange is not significant [Begovic and Copin-Montegut, 2002]. Over the period
148 2013-2015, the CO_2 air-sea flux from the atmosphere to the ocean surface is equal to -0.45
149 $\text{mol m}^{-2} \text{yr}^{-1}$.

150 During summer 2014, large differences between measurements at 3 and 10 meters were
151 observed (Fig. 2, a, b, c between dashed lines). A detailed analysis of the temporal
152 variability during that period underscores the role of inertial waves at the frequency of
153 17.4 hours that create the observed differences between the 2 depths of observations,
154 the deeper waters being colder and enriched in $f\text{CO}_2@13$. T and $f\text{CO}_2@13$ variability is
155 dominated by inertial waves. In particular, from 15 to 26 of August 2014, the difference
156 in T between the two depths is as large as 7.6°C , and 5.1°C on average. $f\text{CO}_2$ decreases on
157 average by $32.7 \mu\text{atm}$ leading to an increase of $f\text{CO}_2@13$ equal to $42.8 \mu\text{atm}$.

158 The 2013-2015 seasonal and inter-annual variability of T, $f\text{CO}_2$ and $f\text{CO}_2@13$ is
159 illustrated on Fig. 2, d, e, f. The larger interannual changes in temperature (Fig.2, d) are
160 observed during summer, both at 3 m and 10 m depth, while over February and March, a
161 constant value of 13°C is observed as the result of vertical mixing with the LIW. A very
162 large inter-annual variability of $f\text{CO}_2@13$ is observed for $T < 14^\circ\text{C}$ (Fig. 2,f). This is
163 associated with the winter mixing at the mooring site, which is highly variable from year
164 to year. Winter mixed-layer depth, MLD, varies between 50 and 160 m, at the top of the
165 LIW over the 2013-2015 period [Coppola *et al.*, 2016]. The variable depth of the winter
166 vertical mixing causes the difference in $f\text{CO}_2@13$ as $f\text{CO}_2$ increases with depth [Copin-
167 Montegut and Begovic, 2002]. The deepening of MLD is driven by episodic and intense

168 mixing processes characterized by a succession of events lasting several days, related to
169 atmospheric forcing [Antoine *et al.*, 2008] which lead to increase in $fCO_2@13$. Figure 2,e
170 illustrates the solubility control of the variability of fCO_2 , as fCO_2 increases when T
171 increases. Another cause of inter-annual variability of fCO_2 for $T\sim 14^\circ C$ is the timing of
172 the spring increase of biological activity which differs by a month between years; for
173 instance, it happened at the beginning of April in 2013, $T\sim 15-16^\circ C$ and by mid March in
174 2014, $T\sim 14^\circ C$. Another cause is the deepening of the mixed layer due to the fall cooling
175 which varies by a month between years.

176

177 3.2 Decadal changes of hydrography

178 3.2.1 Sea surface temperature changes

179 Monthly mean values of temperature have been computed for the two three-year periods,
180 1995-1997 and 2013-2015. In 1995-1997, fCO_2 and T at 2 m were measured with CARIOCA
181 sensors installed on a buoy at DYFAMED [Hood and Merlivat, 2001]. The mean annual
182 temperature of hourly CARIOCA data is equal to $18.21^\circ C$. For 2013-2015, temperature
183 measurements made on the BOUSSOLE mooring at 3 and 10 meters have been used. For the
184 April to September time interval, there are only data at 3m depth. In addition, temperature
185 data measured half hourly at 0.7 m at a nearby meteorological buoy ($43^\circ 23' N$, $7^\circ 50' E$)
186 (<http://www.meteo.shom.fr/real-time/html/DYFAMED.html>) have been used (Fig.3d). Mean
187 annual temperature are equal to $18.29^\circ C$ and $17.97^\circ C$ respectively, based on the
188 meteorological buoy and the BOUSSOLE mooring data. The two sets of data differ
189 essentially during July and August, with the temperatures at 3 m being colder than at 0.7 m,
190 indicating a thermal gradient between the two depths during summer. Therefore, for 2013-
191 2015, we select the mean annual value computed with the meteorological buoy, $18.29^\circ C$, as
192 better representing the sea surface. This value is very close to $18.21^\circ C$ computed for 1995-
193 1997. Then, no significant change of SST is found between the 2 decades, with a mean value
194 equal to $18.25^\circ C$.

195 3.2.2 Sea surface salinity changes

196 The mean value of salinity computed from 56 samples taken at BOUSSOLE in 2013-2015 is
197 equal to 38.19 ± 0.14 . In 1998-1999, ship measurements of surface salinity were made during
198 monthly cruises at the DYFAMED site [Copin-Montégut *et al.*, 2004]. The mean salinity of
199 this set of 19 data is equal to 38.21 ± 0.12 . Thus, there is no significant salinity change
200 between the two decades.

201

202 3.3 Decadal changes of $f\text{CO}_2@13$

203 3.3.1 Time series of $f\text{CO}_2@13$ in 1995-1997 and 2013-2015

204 The two time series of high frequency data were analyzed in order to quantify the change of
205 $f\text{CO}_2@13$ at the sea surface two decades apart. To account for the interannual seasonal
206 variability as well as irregular sampling, we performed an analysis of the change of $f\text{CO}_2@13$
207 as a function of SST (Fig. 3, a and b). For the 2013-2015 data set, we excluded summer data
208 measured at 10 m depth as they were not representative of the surface mixed layer due to a
209 strong stratification. Much larger $f\text{CO}_2@13$ values are observed at low temperature than at
210 high temperature, the decrease being similar for the two studied periods and strongly non
211 linear. As described in section 3.1, large values at low temperature result from mixing with
212 enriched deep waters during winter and low values for 26°C-28°C temperatures occur at the
213 end of summer after biological drawdown of carbon. An increase of $f\text{CO}_2@13$ between the 2
214 periods is clearly highlighted for the whole range of temperature.

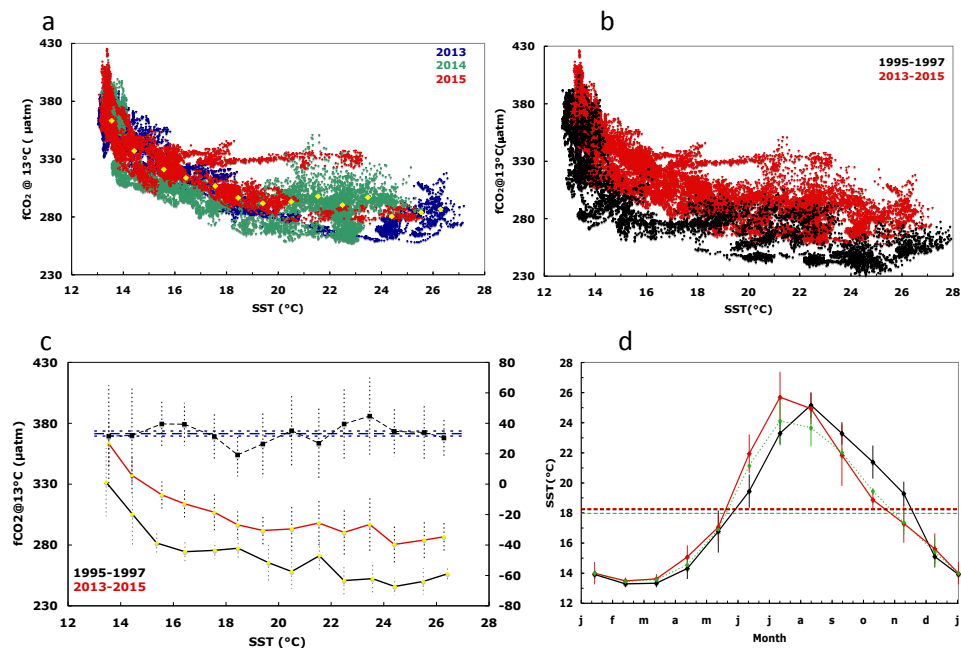


Fig.3. (a) $f\text{CO}_2@13^\circ\text{C}$ as a function of temperature for hourly data in 2013, 2014 and 2015. The yellow dots indicate mean $f\text{CO}_2@13^\circ\text{C}$ (b) as in (a) but for all hourly data in 1995-1997 (black) and in 2013-2015 (red) (c) As in (b), but for average values per 1°C interval (standard deviation as dotted line). The difference between the two periods is also displayed (dashed black curve; scale on the right axis). (d) Mean monthly sea surface temperature for 1993-1995 (black curve; CARIOCA sensors), 2013-2015 (green; CARIOCA sensors), 2013-2015 (red, meteorological buoy). Corresponding mean annual values are indicated by dotted lines.

215

216 3.3.2 Trend analysis and statistics

217 To quantify the change of fCO₂@13 between the two data sets, we proceed as follows: data
 218 are binned by 1°C temperature intervals, thereby removing any potential seasonal weighting,
 219 especially towards the 13-14°C winter months temperature. The measurements made in this
 220 temperature interval represent about 25% of the total number of data for both periods. For
 221 each of the fourteen 1°C step, the mean and standard deviation of hourly fCO₂@13
 222 measurements are reported in Table 1 and on Fig. 3c.
 223

Time interval 1995-1997				Time interval 2013-2015				Temporal trend	
T °C	fCO ₂ @13 µatm	N	standard deviation µatm	T °C	fCO ₂ @1 3 µatm	N	standard deviation µatm	dfCO 2@13 µatm	standard deviation µatm
13.45	331.58	1212	28.09	13.55	363.14	6869	18.07	31.56	33.40
14.45	305.28	495	26.02	14.43	337.16	3270	16.65	31.87	30.89
15.37	281.54	447	9.62	15.57	321.10	3112	11.09	39.56	14.68
16.44	274.43	182	8.53	16.42	313.79	1818	11.09	39.36	13.99
17.58	275.54	190	7.04	17.56	306.83	1528	14.65	31.29	16.25
18.47	277.34	300	9.04	18.45	296.57	2621	10.95	19.23	14.20
19.62	265.43	342	15.58	19.41	291.84	1406	13.45	26.40	20.59
20.50	258.08	529	14.15	20.50	293.16	1135	18.21	35.08	23.06
21.56	271.15	239	12.98	21.54	297.96	1200	20.41	26.82	24.19
22.49	250.75	742	13.66	22.49	290.27	2385	18.57	39.52	23.05
23.57	252.22	320	13.00	23.47	296.92	747	21.77	44.70	25.36
24.41	245.85	506	7.08	24.40	280.44	959	14.82	34.59	16.43
25.50	250.06	215	10.77	25.53	284.05	456	14.81	33.99	18.31
26.42	256.29	279	6.24	26.29	286.71	249	11.23	30.42	12.85

224

225

Table 1:

226 Distribution of temperature, fCO₂@13, and increase dfCO₂@13 data binned by 1°C
 227 temperature interval for the 2 periods 1995-1997 and 2013-2015 .

228 The mean temperature within each 1° step differ for the two periods as the distribution of
 229 individual measurements are not identical.

230 For both data sets, a monotonic relationship between $f\text{CO}_2@13$ and T is observed with
231 correlation coefficients respectively equal to -0.861 and -0.857. The difference in $f\text{CO}_2@13$
232 between the two periods, $df\text{CO}_2@13$, is derived in each temperature step, as the difference
233 between column 2 and 6 of Table 1. The variability of this difference is estimated as the
234 quadratic mean of the standard deviation in each time series. Both values are reported in
235 Table 1, column 9 and 10, and on Fig. 3c.

236 It is interesting to note that the distribution of values around the mean seems random
237 and indicates no trend dependency with SST (Fig. 3c). This suggests that the processes
238 which control the seasonal variation of $f\text{CO}_2@13$ at the sea surface have not changed
239 over the last two decades. The mean weighted value of $df\text{CO}_2@13$ over the whole range of
240 temperature is estimated as the mean of $df\text{CO}_2@13$ in each temperature step weighted by the
241 variance. It is equal to $32.7\mu\text{atm}$. We estimate the accuracy on this value as follows. For each
242 time interval, the mean $f\text{CO}_2@13$ per temperature step has been derived from at least three
243 independent CARIOCA sensors. Given that the accuracy on $f\text{CO}_2$ from each CARIOCA
244 sensor is estimated at $2\mu\text{atm}$ and that the calibrations of the three sensors are independent,
245 the accuracy on $f\text{CO}_2$ averaged in each time interval is $2/\sqrt{3}=1.15\mu\text{atm}$. Hence the accuracy
246 on the difference is estimated at $1.6\mu\text{atm}$.

247

248 **3.4 Changes of seawater carbonate chemistry in surface waters**

249 We estimated the DIC and pH changes related to the increase of $f\text{CO}_2@13$ measured at the
250 sea surface 18 years apart, assuming a mean salinity equal to 38.2, a mean alkalinity equal to
251 $2562.3\mu\text{mol kg}^{-1}$ following equation (1), and a mean in situ temperature, T, equal to 18.25°C .
252 The dissociation constants of Mehrbach refitted by Dickson and Millero [*Dickson and*
253 *Millero, 1987; Mehrbach et al., 1973*] were used. pH is calculated on the seawater scale. We
254 compute an increase of DIC, $d\text{DIC}$, equal to $24.8\pm 1.3\mu\text{mol kg}^{-1}$ ($1.38\pm 0.07\mu\text{mol kg}^{-1}\text{yr}^{-1}$)
255 and the decrease of pH, $dp\text{H}$ equal to -0.0390 ± 0.0020 pH unit ($-0.0022\pm 0.0001\text{pH unit yr}^{-1}$)
256 ¹⁾ (Table 2).

	d fCO ₂ * @ 13°C µatm	d fCO ₂ * @ T µatm	d DIC* µmolkg ⁻¹	d pH* pH unit	dfCO ₂ @T annual µatm yr ⁻¹	d DIC annual µmolkg ⁻¹ yr ⁻¹	d pH annual pH unit yr ⁻¹
sea surface	32.7 +/-1.6	40.8 +/-2.0	24.8 +/-1.3	-0.0390 +/-0.0020	2.27 +/-0.11	1.38 +/-0.07	-0.0022 +/-0.0001
atmosphere Lampedusa data		34.3 +/-1.2	**20.8 +/-0.8		1.91 +/-0.07		
dfCO ₂ @T _{air} /dfCO ₂ @T _{sea}		0.84 +/-0.05					

257

258

Table 2

259 Seasonally detrended long term and annual trends of seawater carbonate chemistry and
260 atmosphere composition.

261 T_{mean} annual temperature equal to 18.25°C

262 *, Change from 1995-1997 to 2013-2015.

263 **, dDIC_{ant}

264

265 3.5 Changes in atmospheric and seawater fCO₂

266 The increase of atmospheric fCO₂ from 1995-1997 to 2013-2015 was computed from the
267 monthly atmospheric xCO₂ concentrations measured at the Lampedusa Island station (Italy)
268 (35°31'N, 12°37'E) (<http://ds.data.jma.go.jp/gmd/wdcgg/>) (see equation 3 in [*Hood and*
269 *Merlivat, 2001*]). Considering a mean annual in situ temperature equal to 18.25°C and an
270 atmospheric pressure equal to 1 atm, we derived a mean atmospheric fCO₂ equal to 355.3+/-
271 0.8 µatm and 389.6+/-0.9 µatm for 1995-1997 and 2013-2015, that is an increase equal to
272 34.3+/-1.2 µatm (Table 2). At this temperature, the change of fCO₂ at the sea surface is equal
273 to 40.8+/-2.0 µatm. Thus the contribution of the increase in atmospheric CO₂ is responsible
274 for 84+/-5 % of the increase of fCO₂ measured in the surface waters. Assuming the same
275 salinity and alkalinity as previously, the corresponding amount of anthropogenic carbon taken
276 up from the atmosphere in order to maintain a chemical equilibrium at the sea surface would
277 be equal to 20.8+/- 0.8 µmol kg⁻¹ (Table 2).

278

279 4 Discussion

280 4.1 fCO₂ at the air-sea interface

281 We have computed that 84% of the increase of $f\text{CO}_2$ _{sea} in the northwestern Mediterranean,
282 two decades apart, comes from the atmosphere. One implicit assumption is that any change in
283 atmospheric $f\text{CO}_2$ immediately transfers as a change in the surface ocean $f\text{CO}_2$. In agreement
284 with the circulation pattern of the basin [Millot, 1999], this increase of surface $f\text{CO}_2$ could
285 follow two routes: in situ chemical equilibrium at the air-sea interface or winter mixing with
286 DIC rich Levantine Intermediate water or surface waters of Atlantic origin, relatively
287 enriched in anthropogenic carbon. Keeping in mind that the deep-water renewal time is
288 estimated to be 20-40 years in the western basin, and given that the atmospheric increase was
289 slower 20-40 years ago, our estimate of the atmospheric contribution to the ocean trend is
290 likely an upper bound.

291 The mean values of $f\text{CO}_2$ computed at the mean annual SST, 18.25°C, computed with all the
292 individual hourly $f\text{CO}_2$ measurements in 1995-1997 and 2013-2015 are respectively equal to
293 352.3 μatm and 400.2 μatm , while the corresponding atmospheric values are 355.3 μatm and
294 389.6 μatm respectively. The CO_2 annual flux is directed from the atmosphere to the sea in
295 both cases, although the annual average of $f\text{CO}_2$ in surface seawater in 2013-2015 is higher
296 than atmospheric $f\text{CO}_2$. This is due to higher wind speed in autumn and winter when the
297 surface water is undersaturated (Fig.2, b).

298

299 4.2 Time change of surface alkalinity?

300 In the range of salinity of the BOUSSOLE samples, 37.9 to 38.5 psu, the alkalinity values
301 computed with Eq (1) are larger than those predicted by the [Copin-Montegut and Begovic,
302 2002] relationship established for the DYFAMED site, with a mean difference equal to 10+/-
303 2 $\mu\text{mol kg}^{-1}$. In both cases alkalinity measurements were made with a potentiometric method
304 using certified reference material supplied by AG Dickson for calibration.

305 It is difficult to identify the cause for a possible change of alkalinity between the 2 periods, 18
306 years apart, while no salinity change has been observed. At a coastal site 50 km away from
307 DYFAMED, [Kapsenberg *et al.*, 2017] have measured an increase of alkalinity unrelated to
308 salinity over the period from 2007 to 2015. They attribute it to changes in freshwater inputs
309 from land. However, based on data from Coppola *et al.*, [2016], alkalinity in the upper 50m at
310 DYFAMED did not change significantly from 2007 through 2014 (3.204 $\mu\text{mol kg}^{-1}$,
311 $P=0.0794$, $r^{*2}=0.08$). Thus, we cannot conclude on whether the difference observed at
312 DYFAMED/BOUSSOLE between the two periods is real or an artifact of measurement
313 techniques. However, as a sensitivity test, if we compute the expected changes of DIC and pH
314 from 1995-1997 to 2013-2015 for a mean alkalinity increase of 10 $\mu\text{mol kg}^{-1}$, we get annual

315 changes, $dDIC=+0.46 \mu\text{mol kg}^{-1}\text{yr}^{-1}$ and $dpH=-0.0001 \text{ pH unit yr}^{-1}$. Such a change in
316 alkalinity does not significantly affect the decrease of pH shown in Table 2.

317

318 4.3 Anthropogenic carbon storage in surface waters

319 The increase of sea surface DIC from 1995-1997 to 2013-2015 is equal to $24.8\pm 1.3 \mu\text{mol}$
320 kg^{-1} (Table 2). ($dDIC_{\text{ant}}$) predicted solely from chemical equilibrium of the sea surface with
321 the atmosphere is equal to $20.8\pm 0.8 \mu\text{mol kg}^{-1}$. The ratio of these two terms is equal to
322 0.84 ± 0.05 . In order to interpret the additional contribution of DIC to that resulting from the
323 local CO_2 air-sea exchange, we examine below two processes, respectively an increased
324 mixing with deep waters and an anthropogenic carbon invasion.

325 MLD time series show a strong variability in winter at interannual scale. During the two
326 periods, 1995-1997 and 2013-2015, the winter MLD never exceeded 220 m, whereas values
327 over 300 m were observed in 1999 and especially in February and March 2006 with values
328 close to 2000 m [Coppola et al., 2016; Pasqueron de Fommervault et al., 2015]. These
329 episodes of strong and deep vertical mixing must have entrained DIC rich LIW in the surface
330 waters. This could be a cause for the observed increase of DIC measured between the two
331 periods 1995 -1997 and 2013-2015.

332 As a result of a monitoring program in the Strait of Gibraltar, [Huertas et al., 2009]
333 calculated a net flux of C_{ant} from the Atlantic towards the Mediterranean basin. [Schneider et
334 al., 2010], using the transit time distribution method applied to a dataset of a Mediterranean
335 cruise in 2001, estimated a net anthropogenic carbon flux across the Strait of Gibraltar into
336 the Mediterranean Sea of 3.5 Tg C yr^{-1} . Over the whole period from 1850 to 2001, this
337 contribution of C_{ant} represents almost 10% of the total C_{ant} inventory of the Mediterranean
338 Sea. Accordingly, about 90% must have been taken directly by equilibrium with atmospheric
339 CO_2 . Based on a high-resolution regional model, [Palmiéri et al., 2015] computed the
340 anthropogenic carbon storage in the Mediterranean basin. They concluded that 75% of the
341 total storage of C_{ant} in the whole basin comes from the atmosphere and 25% from net
342 transport from the Atlantic across the Strait of Gibraltar. The findings of these two studies
343 support the conclusion that computed change of DIC in excess of $16\pm 5\%$ over the direct
344 contribution of air-sea exchange could result from the anthropogenic carbon input from the
345 Atlantic Ocean towards the Mediterranean basin. [Huertas et al., 2009] and [Schneider et al.,
346 2010] report DIC_{ant} surface concentrations respectively equal to $65\text{-}70 \mu\text{mol kg}^{-1}$ at the strait
347 of Gibraltar in the years 2005-2007 and close to $65 \mu\text{mol kg}^{-1}$ in the western basin in 2001.
348 We extrapolate these figures to the year 2014, assuming a mean increase rate of DIC equal to

349 1.38 $\mu\text{mol kg}^{-1}\text{yr}^{-1}$ as previously computed (Table 2). Taking into account the increase of
350 DIC_{ant} equal to 24.8 $\mu\text{mol kg}^{-1}$ between 1995-1997 and 2013-2015, we would estimate that
351 the contribution of the change of DIC_{ant} over the last 18 years represents $\sim 30\%$ of the total
352 change since the beginning of the industrial period ($t > \sim 1800$).

353

354 4.4 The signal of acidification

355 The annual decrease of pH_T calculated between 1995-1997 and 2013-2015 is equal to -
356 0.0022 ± 0.0001 . At the DYFAMED site, at 10 m depth, [Marcellin Yao *et al.*, 2016] studied
357 the time variability of pH over 1995-2011, based on measurements of T, S, Alk and DIC
358 sampled approximately once a month. They computed a mean annual decrease of $-0.003 \pm$
359 0.001 pH units on the seawater scale that is not significantly different from our estimate.
360 [Bates *et al.*, 2014] examined changes in surface seawater CO_2 -carbonate chemistry at the
361 locations of seven ocean CO_2 time series that have been gathering sustained observations
362 from 15 to 30 years with monthly or seasonal sampling. The range of decreasing trends of pH
363 extends from -0.0026 ± 0.0006 unit yr^{-1} at the Irminger Sea time series site to $-0.0014 \pm$
364 0.0005 unit yr^{-1} at the Iceland Sea time series. For the global surface ocean, [Lauvset *et al.*,
365 2015] have reported a mean rate of decrease of -0.0018 ± 0.0004 for 1991-2011. The decrease
366 of pH computed here at DYFAMED is in the upper range of values compared to other time
367 series. The waters of the Mediterranean Sea have a relatively high absorption capacity to
368 absorb anthropogenic carbon for two reasons, the decrease of the Revelle factor, close to ten,
369 because of the high values of the alkalinity and the relatively short deep water renewal time
370 estimated to be 20-40 years in the western basin [Schneider *et al.*, 2010].

371

372 5 Conclusion

373 High-frequency ocean fCO_2 measurements made by CARIOCA sensors were sufficient to
374 estimate trends in fCO_2 , DIC and pH over a period of two decades, notwithstanding a
375 considerable short-time and natural seasonal variability of these properties at the sea surface.
376 We have estimated a large change of sea surface carbonate chemistry, an increase of DIC and
377 a decrease of pH. The computed increase of DIC is larger than the change expected from
378 chemical equilibrium with atmospheric CO_2 . This could be the result of a strong interannual
379 variability of the winter mixing as observed between the two periods 1993-1995 and 2013-
380 2015. Likewise, our results support modeling work and analysis of vertical profiles
381 measurements that suggest that the Atlantic Ocean contributes as a source of anthropogenic
382 carbon towards the Mediterranean basin, close to 10% ([Schneider *et al.*, 2010] or 25%

383 [Palmiéri et al., 2015].

384

385 *Data availability:* Time series data from Dyfamed (1995-1997) are available in the SOCAT v3
386 database. Boussole data (2013-2015) will be available in SOCAT v6.

387

388 **Acknowledgments**

389 Seawater samples were analyzed for DIC and Alk by the SNAPO-CO₂ at LOCEAN in Paris.
390 The CO₂Sys toolbox of [Pierrot et al., 2006] has been used for the calculations of DIC and
391 pH. The adaptation of CARIOCA sensors to high pressure has been supported by the BIO-
392 optics and CARbon EXperiment (BIOCAREX) project, funded by the Agence Nationale de la
393 Recherche (ANR, Paris). We are grateful for helpful comments from Gilles Reverdin on the
394 manuscript. Many thanks to Laurent Coppola who kindly provided additional MLD data at
395 Dyfamed.

396

397 **References**

398

399 Antoine, D., F. d'Ortenzio, S. B. Hooker, G. Bécu, B. Gentili, D. Tailliez, and A. J. Scott
400 (2008), Assessment of uncertainty in the ocean reflectance determined by three satellite
401 ocean color sensors (MERIS, SeaWiFS and MODIS-A) at an offshore site in the
402 Mediterranean Sea (BOUSSOLE project), *Journal of Geophysical Research*, 113(C7).

403 Antoine., and others (2006), BOUSSOLE: A Joint CNRS-INSU,ESA, CNES and NASA ocean
404 color calibration and validation activity., *NASA Tech. Memo. 2006-214147*.

405 Bakker, D. C. E., et al. (2014), An update to the Surface Ocean CO₂ Atlas
406 (SOCAT version 2), *Earth Syst. Sci. Data*, 6(1), 69-90.

407 Bates, N., Y. Astor, M. Church, K. Currie, J. Dore, M. Gonaález-Dávila, L. Lorenzoni, F.
408 Muller-Karger, J. Olafsson, and M. Santa-Casiano (2014), A Time-Series View of Changing
409 Ocean Chemistry Due to Ocean Uptake of Anthropogenic CO₂ and Ocean Acidification,
410 *Oceanography*, 27(1), 126-141.

411 Begovic , M., and C. Copin-Montegut (2002), Processes controlling annual variations in
412 the partial pressure of fCO₂ in surface waters of the central northwestern
413 Mediterranean sea (Dyfamed site), *Deep-Sea Research II*, 49, 2031-2047.

414 Chen, G. T., and F. J. Millero (1979), Gradual increase of oceanic CO₂, *Nature*, 277, 205-
415 206.

416 Copin-Montegut, C., and M. Begovic (2002), Distributions of carbonate properties and
417 oxygen along the water column (0–2000 m) in the central part of the NW Mediterranean
418 Sea (Dyfamed site): influence of winter vertical mixing on air–sea CO₂ and O₂
419 exchanges, *Deep-Sea Research II* 49, 2049-2066.

420 Copin-Montégut, C., M. Bégovic, and L. Merlivat (2004), Variability of the partial pressure
421 of CO₂ on diel to annual time scales in the Northwestern Mediterranean Sea, *Mar Chem*,
422 85(3-4), 169-189.

423 Coppola, L., E. Diamond Riquier, and T. Carval (2016), Dyfamed observatory data,
424 *SEANOE*.

425 Dickson, A. G., and F. J. Millero (1987), A comparison of the equilibrium constants for the
426 dissociation of carbonic acid in seawater media, *Deep Sea Research Part A*.
427 *Oceanographic Research Papers*, 34(10), 1733-1743.

428 Edmond, J. M. (1970), High precision determination of titration alkalinity and total
429 carbon dioxide content of seawater by potentiometric titration, *Deep Sea research* 17(4),
430 737-750.

431 Gattuso, J.-P., and L. Hansson (2011), Ocean Acidification, *Oxford University Press*, 352
432 pp.

433 Gruber, N., J. L. Sarmiento, and T. F. Stocker (1996), An improved method for detecting
434 anthropogenic CO₂ in the oceans, *Global Biogeochem Cy*, 10, 809-837.

435 Heimbürger, L.-E., H. Lavigne, C. Migon, F. D'Ortenzio, C. Estournel, L. Coppola, and J.-C.
436 Miquel (2013), Temporal variability of vertical export flux at the DYFAMED time-series
437 station (Northwestern Mediterranean Sea), *Progress In Oceanography*, 119, 59-67.

438 Hood, E. M., and L. Merlivat (2001), Annual and interannual variations of fCO₂ in the
439 northwestern Mediterranean Sea: Results from hourly measurements made by CARIOCA
440 buoys, 1995-1997, *J Mar Res*, 59, 113-131.

441 Huertas, I. E., A. F. Ríos, J. García-Lafuente, A. Makaoui, S. ` Rodríguez-Gálvez, A. Sánchez-
442 Román, A. Orbi, J. Ruíz, and F. F. and Pérez (2009), Anthropogenic and natural CO₂
443 exchange through the Strait of Gibraltar, *Biogeosciences*, 6, 647-662.

444 Kapsenberg, L., S. Alliouane, F. Gazeau, L. Mousseau, and J.-P. Gattuso (2017), Coastal
445 ocean acidification and increasing total alkalinity in the northwestern Mediterranean
446 Sea, *Ocean Science*, 13(3), 411-426.

447 Lauvset, S. K., N. Gruber, P. Landschützer, A. Olsen, and J. Tjiputra (2015), Trends and
448 drivers in global surface ocean pH over the past 3 decades, *Biogeosciences*, 12(5), 1285-
449 1298.

450 Marcellin Yao, K., O. Marcou, C. Goyet, V. Guglielmi, F. Touratier, and J.-P. Savy (2016),
451 Time variability of the north-western Mediterranean Sea pH over 1995–2011, *Marine*
452 *Environmental Research*, 116, 51-60.

453 Marty, J. C., J. Chiaverini, M. Pizay, D., and B. Avril (2002), Seasonal and interannual
454 dynamics of nutrients and phytoplankton pigments in the western Mediterranean Sea at
455 the DYFAMED time-series station (1991–1999), *Deep-Sea Research II*, 49, 1965-1985.

456 McKinley, G. A., A. R. Fay, T. Takahashi, and N. Metzl (2011), Convergence of
457 atmospheric and North Atlantic carbon dioxide trends on multidecadal timescales,
458 *Nature Geoscience*, 4, 606-610.

459 Mehrbach, C., C. H. Culbertson, J. E. Hawley, and R. M. Pytkowicz (1973), Measurement of
460 the apparent dissociation constants of carbonic acid in seawater at atmospheric
461 pressure, *Limnol Oceanogr*, 18(6), 897-907.

462 Merlivat, L., and P. Brault (1995), CARIOCA BUOY: Carbon Dioxide Monitor, *Sea*
463 *Technol*(October), 23-30.

464 Millero, F. J. (2007), The marine inorganic carbon cycle, *Chemical reviews*, 107(2), 308-
465 341.

466 Millot (1999), Circulation in the Western Mediterranean Sea, *Journal of Marine Systems*,
467 20, 423–442.

468 Palmiéri, J., J. C. Orr, J. C. Dutay, K. Béranger, A. Schneider, J. Beuvier, and S. Somot
469 (2015), Simulated anthropogenic CO₂ storage and acidification of the Mediterranean
470 Sea, *Biogeosciences*, 12(3), 781-802.

471 Pasqueron de Fommervault, O., C. Migon, F. D’Ortenzio, M. Ribera d’Alcalà, and L.
472 Coppola (2015), Temporal variability of nutrient concentrations in the northwestern
473 Mediterranean sea (DYFAMED time-series station), *Deep Sea Research Part I:*
474 *Oceanographic Research Papers*, 100, 1-12.

475 Pierrot, D., E. Lewis, and D. W. R. Wallace (2006), MS excel program developed for CO₂
476 system calculations, *In: Carbon Dioxide Information Analysis Center (ed.O.R.N.L.).*
477 *US.Department of Energy, Oak Ridge, TN.*

478 Sabine, C. L., R. A. Feely, F. J. Millero, A. G. Dickson, C. Langdon, S. Mecking, and D. Greeley
479 (2008), Decadal changes in Pacific carbon, *J.Geophys.Res.*, 113(C07021).

480 Schneider, A., T. Tanhua, A. Körtzinger, and D. W. R. Wallace (2010), High anthropogenic
481 carbon content in the eastern Mediterranean, *Journal of Geophysical Research*, 115(C12).
482 Takahashi, T., J. Olafson, J. G. Goddard, D. W. Chipman, and G. Sutherland (1993),
483 Seasonal variations of CO₂ and nutrients in the high-latitude surface oceans: a
484 comparative study, *Global Biogeochem Cy*, 7(4), 843-878.
485 Touratier, F., and C. Goyet (2004), Applying the new TrOCA approach to assess the
486 distribution of anthropogenic CO₂ in the Atlantic Ocean, *Journal of Marine Systems*, 46(1-
487 4), 181-197.
488 Touratier, F., and C. Goyet (2009), Decadal evolution of anthropogenic CO₂ in the
489 northwestern Mediterranean Sea from the mid-1990s to the mid-2000s, *Deep Sea*
490 *Research Part I: Oceanographic Research Papers*, 56(10), 1708-1716.
491 Woosley, R. J., F. J. Millero, and R. Wanninkhof (2016), Rapid anthropogenic changes in
492 CO₂ and pH in the Atlantic Ocean: 2003-2014, *Global Biogeochem Cy*, 30(1), 70-90.
493
494
495

495
496
497
498
499
500
501
502
503
504
505
506
507
508
509
510
511
512
513
514
515
516
517
518
519
520
521
522
523
524
525
526
527
528

Figure caption and tables

Figure 1. The area of the northwestern Mediterranean Sea showing the southern coast of France, the Island of Corsica, the main current branches (gray arrows), and the location of the DYFAMED site (43°25'N, 7°52'E, red star) and the BOUSSOLE buoy (43°22'N, 7°54'E, black star) in the Ligurian Sea.

Figure 2. Interannual variability of CARIOCA data: a) T, b) fCO₂, c) fCO₂@13. The dotted lines indicate the period affected by stratification and internal waves (July, 26th to October 1st, 2014 and July, 8th to October 1st, 2015). On 2(b), the open circles correspond to fCO₂ data derived from DIC and alkalinity measurements of samples taken at 5 and 10 meters. (d), (e), (f), seasonal variability. On 2(e), the thin lines indicate fCO_{2atm}. Note that the color code on (d), (e), (f) is different from (a), (b), (c).

Figure 3. (a) fCO₂@13 as a function of temperature for hourly data in 2013, 2014 and 2015. The yellow dots indicate mean fCO₂@13 (b) as in (a) but for all hourly data in 1995-1997 (black) and in 2013-2015 (red) (c) As in (b), but for average values per 1°C interval (standard deviation as dotted line). The difference between the two periods is also displayed (dashed black curve; scale on the right axis). (d) Mean monthly sea surface temperature for 1993-1995 (black curve; CARIOCA sensors), 2013-2015 (green; CARIOCA sensors), 2013-2015 (red, meteorological buoy). Corresponding mean annual values are indicated by dotted lines.

Table 1:

Distribution of temperature, fCO₂@13, and increase dfCO₂@13 data binned by 1°C temperature interval for the 2 periods 1995-1997 and 2013-2015 .

The mean temperature within each 1° step differ for the two periods as the distribution of individual measurements are not identical.

Table 2

Seasonally detrended long term and annual trends of seawater carbonate chemistry and atmosphere composition.

T, mean annual temperature equal to 18.25°C

*, Change from 1995-1997 to 2013-2015.

**, dDIC_{ant}